



Original Article



# Sarmentosin Induces Autophagy-dependent Apoptosis via Activation of Nrf2 in Hepatocellular Carcinoma

Zhitao Jiang<sup>1#</sup>, Liyuan Gao<sup>1#</sup>, Chundi Liu<sup>1</sup>, Jianchun Wang<sup>1</sup>, Yi Han<sup>1</sup> and Jinhua Pan<sup>2#\*</sup>

<sup>1</sup>Department of Pharmacy, Zhangjiagang Hospital of Traditional Chinese Medicine Affiliated to Nanjing University of Chinese Medicine, Zhangjiagang, Jiangsu, China; <sup>2</sup>School of Pharmacy, Nanjing University of Chinese Medicine, Nanjing, Jiangsu, China

Received: 3 July 2022 | Revised: 16 September 2022 | Accepted: 14 October 2022 | Published online: 31 January 2023

## Abstract

**Background and Aims:** Hepatocellular carcinoma (HCC) is a common and deadly cancer. Accumulating evidence supports modulation of autophagy as a novel approach for determining cancer cell fate. The aim of this study to evaluate the effectiveness of sarmentosin, a natural compound, on HCC *in vitro* and *in vivo* and elucidated the underlying mechanisms. **Methods:** Cell functions and signaling pathways were analyzed in HepG2 cells using western blotting, real-time PCR, siRNA, transmission electron microscopy and flow cytometry. BALB/c nude mice were injected with HepG2 cells to produce a xenograft tumour nude mouse model for *in vivo* assessments and their tumors, hearts, lungs and kidneys were isolated. **Results:** We found that autophagy was induced by sarmentosin in a concentration- and time-dependent manner in human HCC HepG2 cells by western blot assays and scanning electron microscopy. Sarmentosin-induced autophagy was abolished by the autophagy inhibitors 3-methyladenine, chloroquine, and bafilomycin A1. Sarmentosin activated Nrf2 in HepG2 cells, as shown by increased nuclear translocation and upregulated expression of Nrf2 target genes. Phosphorylation of mTOR was also inhibited by sarmentosin. Sarmentosin stimulated caspase-dependent apoptosis in HepG2 cells, which was impaired by silencing Nrf2 or chloroquine or knocking down ATG7. Finally, sarmentosin effectively repressed HCC growth in xenograft nude mice and activated autophagy and apoptosis in HCC tissues. **Conclusions:** This study showed sarmentosin stimulated autophagic and caspase-dependent apoptosis in HCC, which required activation of Nrf2 and inhibition of mTOR. Our research supports Nrf2 as a therapeutic target for HCC and sarmentosin as a promising candidate for HCC chemotherapy.

**Citation of this article:** Jiang Z, Gao L, Liu C, Wang J, Han Y, Pan J. Sarmentosin Induces Autophagy-dependent Apoptosis via Activation of Nrf2 in Hepatocellular Carcinoma.

**Keywords:** Hepatocellular carcinoma; Sarmentosin; Autophagy; Apoptosis; Nrf2.

**Abbreviations:** ATG, autophagy-related gene; Baf A1, bafilomycin A1; CQ, chloroquine; HCC, hepatocellular carcinoma; HE, hematoxylin-eosin; LC3B, microtubule-associated protein 1 light chain 3B; 3-MA, 3-methyladenine.

\*Contributed equally to this work.

**Correspondence to:** Jinhua Pan, Nanjing University of Chinese Medicine, Nanjing, Jiangsu, China. ORCID: <https://orcid.org/0000-0002-0574-192X>. Tel/Fax: +86-512-56380623, E-mail: [panjinhuonj@163.com](mailto:panjinhuonj@163.com)

J Clin Transl Hepatol 2023;11(4):863–876. doi: 10.14218/JCTH.2022.00312.

## Introduction

Hepatocellular carcinoma (HCC) is one of the most common causes of malignant tumor-related mortality worldwide.<sup>1</sup> It is often associated with cirrhosis and liver failure, making the treatment of HCC more difficult than many other cancers. Although chemotherapy, surgery, and radiotherapy have been used alone or in combination for HCC, a majority of HCC patients still have a poor prognosis. The high incidence of recurrence and metastasis makes the overall 5-year survival rate of HCC very low.<sup>2</sup> Chemotherapy has a crucial role in the treatment of HCC, especially at advanced stages. However, apoptotic resistance hampers the efficacy of chemotherapeutic drugs.<sup>3</sup> Thus, increasing attention has been given to developing innovative compounds that increase the death of therapy-resistant HCC cells.

Apoptosis and autophagy are both programmed cell death processes. Unlike apoptosis, which ends in cell death, autophagy exhibits bidirectional roles in cell destiny determination depending on the intensity and duration of inducers.<sup>4</sup> Autophagy is an evolutionarily conserved eukaryotic cell stress mechanism characterized by increased generation of autophagic vesicles with incorporation of long-lived proteins and damaged organelles that are digested in lysosomes.<sup>5</sup> Natural products isolated from traditional Chinese medicines are important sources of anticancer drugs or adjuvant chemotherapy drugs. A previous study showed that extracts of the Chinese medicinal herb *Sedum sarmentosum* prevented D-GalN/LPS-induced fulminant hepatic failure, and protection was associated with modulation of apoptosis,<sup>6</sup> indicating that its active ingredients had the potential to combat liver diseases. Sarmentosin is an unsaturated  $\gamma$ -hydroxynitrile glucoside derived from *Sedum sarmentosum*.<sup>7</sup> The mechanism of the sarmentosin hepatoprotection is not clear and deserves further exploration.

Moderate and controlled autophagy can help cells adapt to stress stimuli such as nutrient deficiency and reactive oxygen species accumulation to promote cell survival.<sup>8</sup> However, excessive autophagy, impairing the cellular constituents and processes, can activate apoptosis and ultimately result in cell death. That process is called autophagic apoptosis, and it de-

depends on cell death stimuli and context.<sup>9</sup> Increasing evidence shows that autophagy is associated with cancer pathogenesis and that pharmacologic manipulation of autophagic machinery may be a novel cancer therapy.<sup>10</sup> The induction of autophagic cell death accounts for the mechanisms of many anticancer reagents.<sup>11</sup> We speculate that sarmentosin functions by regulating autophagy, but evidence is lacking. This study aimed to evaluate the anti-HCC effectiveness and safety of sarmentosin and to elucidate the underlying mechanisms in *in vitro* and *in vivo* systems.

## Methods

### Chemicals and antibodies

Sarmentosin (#CFN97202, C<sub>11</sub>H<sub>17</sub>NO<sub>7</sub>, ≥98%) was purchased from ChemFaces Biochemical Co., Ltd. Wuhan, China. VAD-fmk (#A1902), rapamycin (#A8167), 3-MA (#A8353), and CQ (#A3542) were purchased from Apex-bio Company, Wuhan, China. Primary antibodies against LC3B (#14600-1-AP), p62 (#ab109012), HO-1 (#10701-1-AP), NQO1 (#11451-1-AP) and Nrf2 (#16396-1-AP) were purchased from Proteintech, Wuhan, China. Antibodies against mTOR (#ab32028), phospho-mTOR (#ab109268), cleaved caspase-9 (#ab2324), cleaved caspase-3 (#ab32042), and cleaved-PARP1 (#ab32064) were purchased from Abcam. The cleaved caspase-8 polyclonal antibody (#YC0011) was purchased from ImmunoWay Biotechnology Company. The ATG7 antibody (#bs-2432R) was purchased from Beijing Boasens Biotechnology Co., Ltd.

### Cell culture and transfection with siRNA

HepG2 cells (#HB-8065) were purchased from the American Type Culture Collection and cultured according to the culture method provided by the American Type Culture Collection. The complete growth medium was 90% Eagle's Minimum Essential Medium (MEM, Gibco, #11095080) and 10% fetal bovine serum (Gibco, #10091148). The transfection solutions of control siRNA, Nrf2 siRNA (Santa Cruz, #sc-37030), and ATG7 siRNA (Santa Cruz, #sc-41447) were prepared according to the manufacturer's instructions. HepG2 cells were washed once with transfection medium quickly. The transfection working solution was then added to the culture plate and covered the HepG2 cells for 6 h of incubation. Then, 20% fetal bovine serum-containing MEM medium was added, and the HepG2 cells were incubated with transfection working solution for 24 h. After discarding the medium, HepG2 cells were incubated with serum-free MEM for 12 h before obtaining the transfected HepG2 cells.

### Transmission electron microscopy

HepG2 cells were cultured and seeded in 6-well plates (Corning, #3516) with 200,000 cells per well. HepG2 cells were incubated with 1640 single medium containing 20 μM sarmentosin for 6 h. After the cells were embedded in agar, the samples were cut into ultrathin sections, fixed with 2.5% glutaraldehyde at 4°C, refixed with osmic acid, and then dehydrated. The dehydrated HepG2 cells were subjected to a gold spray conductive treatment, and the processed samples were placed on a copper mesh to photograph the autophagosomes in HepG2 cells using a transmission electron microscope (Hitachi, HT7800).

### Adenovirus expressing mCherry-GFP-LC3B assay

HepG2 cells were cultured and seeded on 24-well plates (Corning, #3524) containing sterile glass slides, with 20,000

cells per well. According to the instructions, HepG2 cells were transfected with Nrf2 siRNA and mCherry-GFP-LC3B adenovirus (Beyotime, #C3012). After incubating for 1 h with or without 3-MA (10 mM), CQ (20 μM), BafA1 (10 nM), or rapamycin (10 nM), the cells were coincubated with 1640 single medium containing 20 μM sarmentosin for 6 or 12 h. HepG2 cells were washed with PBS, and the cells were fixed with 4% paraformaldehyde for 30 min at room temperature. Subsequently, the glass slide containing the cells was removed, and anti-fluorescence quenching mounting solution was added dropwise. A fluorescence microscope (Leica, DMI3000B) was used to take pictures.

### Cell viability assay

HepG2 cells were cultured and seeded on 96-well plates (Corning, #3599) at 5,000 cells/well and cultured for 24 h. Then, the original complete medium was discarded. After incubating for 1 h with or without 3-MA (10 mM), CQ (20 μM), or BafA1 (10 nM), the cells were coincubated in 1640 single medium containing different concentrations of sarmentosin for different durations. Cells were photographed with an inverted optical microscope (Leica, DMI3000B). Then, 20 μL of 5 mg/mL MTT (Beyotime, #ST316) solution was added to each well. After 4 h of incubation, the solution in the wells was discarded. Then, 200 μL of dimethyl sulfoxide (DMSO, Thermo Fisher Scientific, #D12345) was added to each well and shaken at low speed in the dark for 10 m, and the optical density (OD) was measured at 492 nm using a microplate reader (Biotek, ELX800). The cell survival rate of the control group was defined as 100%. A survival curve was plotted using the cell survival rate and the concentrations of sarmentosin to obtain the IC<sub>50</sub> values.

### Cell colony-forming assay

HepG2 cells transfected with Nrf2 siRNA or ATG7 siRNA were digested with 0.25% trypsin (Thermo Fisher Scientific, #25300054) and disaggregated into single cells by pipetting. Cells were added to the 24-well plates at 100 cells/well, and 1 mL of 37°C prewarmed culture medium was added. After incubating cells with or without CQ (20 μM) or Z-VAD-fmk (10 mM) for 1 h, 1640 complete medium containing different concentrations of sarmentosin (10, 20, 30 μM) was added to HepG2 cells in 24-well plates. When macroscopic clones appeared in the dish, the culture was terminated. The cells were immersed in PBS and then fixed using paraformaldehyde (Biosharp, #BL539A) for 20 min. After discarding the fixing solution, the cells were stained for 10 m by adding a proper amount of Giemsa staining solution (Sigma-Aldrich, #48900), immersed in PBS and air-dried. The number of clones larger than 10 cells was counted in a 24-well plate by low magnification light microscopy (Olympus, CX43), and a digital camera (Mshot, MD50) was used to take the pictures.

### Flow cytometry

HepG2 cells transfected with Nrf2 siRNA or ATG7 siRNA in logarithmic growth phase were digested with 0.25% trypsin and pipetted into single cells. Cells were added to 6-well plates at 200,000 cells/well, and 2 mL of 37°C prewarmed culture medium was added. After incubating cells with or without CQ (20 μM) or Z-VAD-fmk (10 mM) for 1 h, 1640 complete medium containing different concentrations of sarmentosin (10, 20, 30 μM) was added to HepG2 cells in 6-well plates. The culture of HepG2 cells was terminated after 12 h. The cells were then centrifuged at 1,000 ×g for 5 m and collected. The cells were gently resuspended in PBS and counted. HepG2 cells (1×10<sup>5</sup>) were centrifuged again, the supernatant was

discarded, and the Annexin V-FITC binding solution and the reaction solution were added. After mixing, the propidium iodide staining solution was added and mixed. After 15 m of incubation in the dark, flow cytometry (BD, Accuri C6) was used to assay apoptosis.

#### **Hoechst staining**

HepG2 cells were cultured and seeded on 24-well plates containing a sterile glass slide, with 20,000 cells per well. HepG2 cells were incubated with 1640 single medium containing 10, 20, or 30  $\mu$ M sarmenosin for 12 h. Then, the cells were washed with PBS and fixed with 4% paraformaldehyde for 30 m at room temperature. The glass slide containing the cells was removed, and Hoechst staining solution (Beyotime, #C1017) was added dropwise and incubated for 20 m. Then, the mounting slide was quenched with anti-fluorescence. Glass slides with HepG2 cells were covered on glass slides and protected from light. A fluorescence microscope (Leica, DMI3000B) was used to take pictures.

#### **Animal procedures and treatment**

Thirty BALB/c nude mice were purchased from Beijing Vital River Experimental Animal Co., Ltd. All animals were kept at the Experimental Animal Use Center of Nanjing University of Chinese Medicine, and the use of animals was approved by the Experimental Animal Ethics Committee of Nanjing University of Chinese Medicine. The experimental animals were kept in an SPF-level experimental animal center. BALB/c nude mice were injected subcutaneously with  $5 \times 10^6$  HepG2 cells in the right flank to produce a xenograft tumor nude mouse model. The mice were divided into five groups: the model group, the 50 mg/kg sarmenosin group, the 100 mg/kg sarmenosin group, the 200 mg/kg sarmenosin group, and the 20 mg/kg 5-FU group. The nude mice were weighed 0, 3, 6, 9, 12, 15, 18, and 21 days after inoculation. Nude mice in the administration groups were given normal saline by intraperitoneal injection once every 3 days. Tumor volume was measured with calipers every 3 days in nude mice in each group, and tumor volume was calculated as length  $\times$  width  $\times$  width. After 21 days, all nude mice were sacrificed, and tumors, hearts, lungs and kidneys were removed. Tumor sections of three mice in each group were frozen, and the remaining organs were fixed in 4% paraformaldehyde.

#### **Hematoxylin and eosin (HE) staining**

Tumor, heart, lung and kidney tissues of the xenograft tumor nude mice were sequentially placed in different concentrations of ethanol (Sinopharm Chemical Reagent, #10009228): 80%, 90%, 95%, and 100%, for 1 h. After dehydration, the tissues were cleared with xylene (Sinopharm Chemical Reagent, #10023418) for 2 h. Tissues were immersed in molten paraffin (Sinopharm Chemical Reagent, #69018961) for 1 h, and tumors, heart, lungs, and kidneys were embedded (Leica, DMI3000B) after changing the paraffin once. The wax blocks were sectioned using a rotary microtome, paraffin wax in the interstitial space was melted, dewaxed with xylene, and then rehydrated, stained with hematoxylin (Beyotime, #C0105) for 4 m, and the sections were washed with tap water for 2 m. The sections were immersed in 1% hydrochloric acid (Sinopharm Chemical Reagent, #10011018, soluble in alcohol) for 20 s, rinsed with water for 20 m, and stained with eosin (Beyotime, #C0105) for 90 s. The sections were soaked in xylene for 10 m after dehydration; the sections were removed, the excess xylene was wiped off, and the coverslips were covered with Kisser's mounting medium (Beyotime, #C1081) for sealing. Tumor, heart, lung and kid-

ney sections were observed and photographed using ordinary light microscopes.

#### **TUNEL staining**

Tumor sections of xenograft tumor nude mouse models were obtained in the same way as for HE staining. After rehydration, the sections were added dropwise to TUNEL staining working solution and incubated for 1 h at room temperature. After washing twice with 0.9% NaCl, the liquid was aspirated. A diaminobenzidine (DAB) kit (Beyotime, #P0202) was used to develop TUNEL-positive spots. Nuclei of tumor sections were counterstained using hematoxylin. After washing, the sections were dehydrated and mounted. The tumor tissue was observed and photographed with a fluorescence microscope (Leica, DMI3000B). The TUNEL-positive area was indicated by brown staining.

#### **Immunohistochemistry**

Tumor sections of xenograft tumor nude mouse models were obtained in the same way as HE staining. Tumor sections were incubated with 3% H<sub>2</sub>O<sub>2</sub> to block endogenous peroxidase in inactivated sections. Antigens for tumor sections were repaired with antigen retrieval solution. All the repaired sections were removed and placed horizontally on an immunohistochemical staining humidifier. The tumor tissue was covered with 5% normal goat serum and incubated at room temperature for 30 m. The primary antibodies and the secondary antibodies were diluted using 5% BSA according to the instructions, and the samples were incubated with primary antibodies against p-mTOR (1:100), ATG7 (1:100), cleaved caspase-3 (1:100), cleaved caspase-8 (1:100), and cleaved caspase-9 (1:100) overnight at 4°C. After washing three times with PBS, 150  $\mu$ L of the secondary antibody was added to the samples and incubated at room temperature for 1 h. After washing three times with PBS, 150  $\mu$ L of DAB color development liquid was added to the samples, and the samples were washed with PBS for 10 m. Nuclei of tumor sections were counterstained using hematoxylin. After washing the sections, the sections were dehydrated and mounted. The tumor tissues were observed and photographed with a common light microscope, and the protein positive expression was brown.

#### **Real-time polymerase chain reaction (PCR)**

Total RNA in HepG2 cells was extracted using TRIzol (Beyotime, #R0016). The cDNA from HepG2 cells was obtained using a reverse transcription kit (TaKaRa, #RR037A) and a PCR instrument (Bio-Rad, T100). The primers for HO-1 and NQO1 were synthesized by Shanghai Biotech Engineering Co., Ltd., and a real-time PCR kit (TaKaRa, #RR820A) was used to perform polymerase chain reaction on an ABI7500 real-time PCR system. GAPDH was an internal control gene. The primer sequences were: HO-1: forward 5'-GAGACGGCTTCAAGCTGGT-GATG-3' and reverse 5'-GTTGAGCAGGAACGCAGTCTTGG-3'; NQO1: forward 5'-AGGCTGGTTGAGCGAGT-3' and reverse 5'-ATTGAATTCGGCGTCTGCTG-3'. The GAPDH primers (Sangon Biotech, #RR037A) were purchased from Shanghai Biotech Engineering Co., Ltd.

#### **Western blotting**

According to the instructions of the Nuclear and Cytoplasmic Protein Extraction Kit (Beyotime, #P0027) or RIPA lysis buffer (Beyotime, #P0013B), samples of HepG2 cells or nude mouse tumors were lysed, and the protein concentrations in the nucleus, cytoplasm and whole cells were determined after total protein was obtained. After the protein samples were

prepared, 50 µg of total protein was taken for SDS-PAGE electrophoresis. The wet transfer method was used to transfer proteins to a PVDF membrane (Millipore, IPVH00010). After blocking, the PVDF membrane was incubated with GAPDH (1:10000), LC3B-I/II (1:500), ATG7 (1:500), p-mTOR (1:1,000), mTOR (1:500), Nrf2 (1:1,000), HO-1 (1:1,000), NQO1 (1:1,000), cleaved caspase-3 (1:1,000), cleaved caspase-8 (1:1,000), cleaved caspase-9 (1:500) and cleaved PARP (1:500) antibodies. After washing the PVDF membrane three times with TBST, the PVDF membrane was incubated with the corresponding secondary antibody (1:10,000) for 2 h. After cleaning the PVDF membrane three times with TBST again, the PVDF membrane was imaged on a gel imaging system (Bio-Rad, ChemiDoc MP) using a high-sensitivity ECL luminescent liquid (Millipore, WBKLS0500).

### Statistical analysis

Western blot data were calculated and exported using Quantity One software. The average OD of immunohistochemistry was calculated and exported using Image-Pro Plus software. The OD of the fluorescence photos was analyzed and exported using ImageJ. Flow cytometry data were analyzed, and data were exported using FlowJo 7.0. The results were reported as means ± SD and were analyzed and graphed using GraphPad Prism 7.0 software. Comparisons among multiple groups were performed by one-way analysis of variance followed by *post hoc* Tukey's test for comparisons between groups. A  $p < 0.05$  was considered statistically significant.

## Results

### Sarmentosin induces autophagy in human HCC cells

We first examined whether sarmentosin affected autophagy in HepG2 cells. Treatment with sarmentosin for 12 h caused morphological changes in a concentration-dependent manner (Fig. 1A). Similar morphological alterations were seen in the cells treated with sarmentosin at 20 µM in a time-dependent manner (Fig. 1B). The effects of sarmentosin on LC3B were examined by western blotting. During autophagy, LC3B-I is converted to LC3B-II, which associates with autophagic vesicles, and the presence of LC3B in autophagosomes and the conversion of LC3B to the lower migrating form LC3B-II have been used as key indicators of autophagy.<sup>12</sup> The results showed that the ratio of LC3B-II/LC3B-I was increased by 12 h of treatment with sarmentosin in a concentration-dependent manner. In addition, p62, as an autophagy substrate, was reduced after sarmentosin treatment (Fig. 1C). Meanwhile, 20 µM sarmentosin also time-dependently increased the LC3B-II/LC3B-I ratio (Fig. 1D). Assays with adenovirus expressing the mCherry-GFP-LC3B fusion protein confirmed that 20 µM sarmentosin induced the formation of autophagosomes in cells (Fig. 1E). Analyses with scanning electron microscopy revealed that autophagic vesicles were increased in sarmentosin-treated cells for 12 h (Fig. 1F). Taken together, the results indicate that sarmentosin stimulated autophagy in human HCC cells.

### Sarmentosin activates autophagic flux in human HCC cells

We next monitored autophagic flux in HepG2 cells treated with sarmentosin using three tool compounds, 3-methyladenine (3-MA), chloroquine (CQ), and bafilomycin A1 (Baf A1) that probe distinct stages of the autophagic process. 3-MA is an inhibitor of class III phosphatidylinositol-3-kinase and prevents the formation of autophagosomes.<sup>13</sup> We saw that pretreatment with 3-MA reversed sarmentosin-induced mor-

phological changes in the cells (Fig. 2A) and that the elevation in the LC3B-II/LC3B-I ratio and the degradation of p62 in sarmentosin-treated cells was abrogated by 3-MA (Fig. 2B). CQ and Baf A1 are lysosomal inhibitors and block lysosome-mediated degradation concomitant with LC3B-II accumulation.<sup>13</sup> We found that the sarmentosin-induced morphological alterations were reversed by pretreatment with CQ or Baf A1 (Fig. 2C). The LC3B-II/LC3B-I ratio was apparently increased by additional pretreatment with CQ or Baf A1 compared with that of sarmentosin treatment alone, and the p62 levels were increased after CQ or Baf A1 treatment (Fig. 2D, E). Assays with adenovirus expressing mCherry-GFP-LC3B fusion protein transfection further revealed that 3-MA abolished the sarmentosin-induced formation of autophagosomes and that CQ and Baf A1 enhanced autophagosome accumulation caused by sarmentosin (Fig. 2F). Collectively, the results indicated that sarmentosin activated autophagic flux in human HCC cells.

### Activation of Nrf2 is required for sarmentosin to inhibit mTOR signaling and induce autophagy in human HCC cells

We next investigated the signaling events underlying sarmentosin-stimulated autophagy. Western blotting analyses of cytoplasmic and nuclear lysates showed that sarmentosin concentration-dependently reduced the abundance of Nrf2 in the cytoplasm and increased the abundance of Nrf2 in the nucleus (Fig. 3A). In addition, sarmentosin increased mRNA and protein expression of HO1 and HQO1 in a concentration-dependent manner, two well-established target genes of Nrf2 (Fig. 3B, C).<sup>15</sup> The data strongly suggested that sarmentosin activated Nrf2 signaling in human HCC cells. Then, mTOR, a pivotal regulator of autophagy, was examined by western blotting, and the results showed that phosphorylation of mTOR was decreased by sarmentosin in a concentration-dependent manner (Fig. 3D), suggesting blockade of mTOR signaling. To verify whether Nrf2 activation was a prerequisite for the effects of sarmentosin, we used knockdown approaches using Nrf2 siRNA transfection. The results showed that siRNA-mediated deficiency of Nrf2 rescued sarmentosin-suppressed mTOR phosphorylation and abolished the sarmentosin-increased LC3B-II/LC3B-I ratio (Fig. 3E). Consistently, assays with adenovirus expressing mCherry-GFP-LC3B fusion protein transfection further revealed that Nrf2 knockdown abolished the sarmentosin-induced formation of autophagosomes (Fig. 3F). To verify the role of mTOR in that setting, the cells were treated with sarmentosin combined with the mTOR inhibitor rapamycin. We saw that rapamycin, like sarmentosin, increased the LC3B-II/LC3B-I ratio, promoted autophagosome formation, and that their combination produced more significant effects (Fig. 3G, H). Altogether, the results suggested that Nrf2 activation is required for sarmentosin inhibition of mTOR signaling and stimulation of autophagy in human HCC cells.

### Sarmentosin stimulates caspase-dependent apoptosis in human HCC cells, which requires activation of Nrf2 and induction of autophagy

We examined the consequences of sarmentosin-induced autophagy. HepG2 cells were treated with sarmentosin for 48 h, which was longer than the time of autophagy induction. MTT assays showed that sarmentosin reduced cell viability in a concentration-dependent manner with an IC<sub>50</sub> of 20.38 µM (Fig. 4A). Cell colony-forming experiments revealed that cell proliferation was also repressed by sarmentosin in a concentration-dependent manner (Fig. 4B). Sarmentosin stimu-

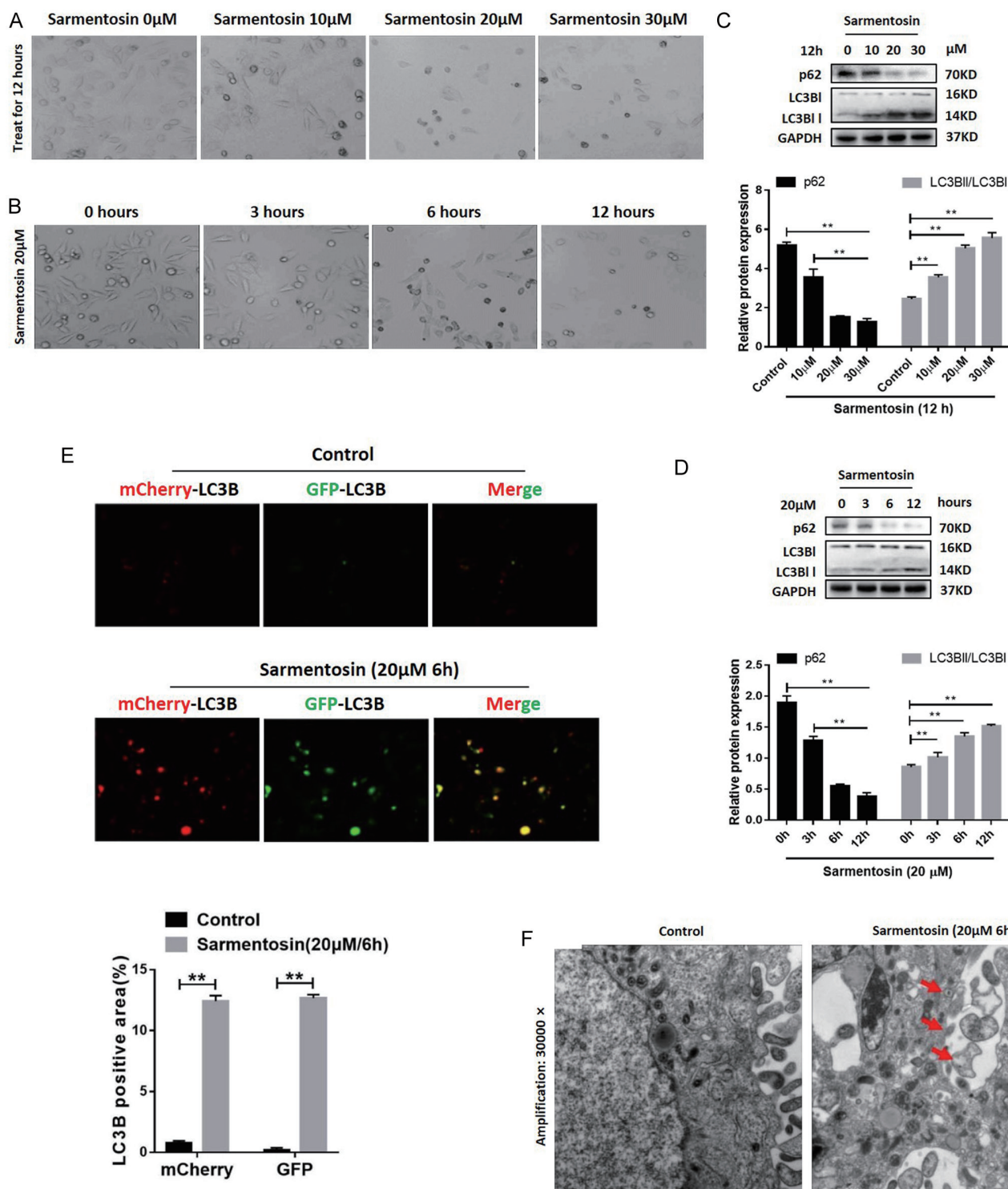


**Fig. 1. Sarmentosin induces autophagy in human HCC cells.** (A) Representative images of HepG2 cells obtained by optical microscopy show the effects of different concentrations of sarmentosin (10, 20, 30 μM) treatment for 12 h on cell morphology and growth. *n*=10. (B) Representative images of HepG2 cells obtained by optical microscopy show the effects of sarmentosin (20 μM) treatment for different times (0, 3, 6, or 12 h) on cell morphology and growth. *n*=10. (C) Western blots and quantitative analysis show changes in LC3BI/II expression in HepG2 cells after 12 h of treatment with different concentrations of sarmentosin (10, 20, 30 μM). *n*=3, \*\**p*<0.01. (D) Western blots and quantitative analysis show changes in LC3BI/II expression in HepG2 cells after treatment with sarmentosin (20 μM) for 0, 3, 6, or 12 h. *n*=3, \*\**p*<0.01. (E) After transfection with mCherry-GFP-LC3B in HepG2 cells, LC3B expression in HepG2 cells in the presence or absence of 6 h of sarmentosin (20 μM) treatment was observed by fluorescence microscopy. The LC3B-positive area percentage was calculated from the fluorescent images. *n*=6, \*\**p*<0.01. (F) Autophagosomes were observed by transmission electron microscopy in HepG2 cells in the presence or absence of 6 h of sarmentosin (20 μM) treatment. Red arrows: autophagosomes, magnification: 30,000×, *n*=3. HCC, hepatocellular carcinoma; LC3B, microtubule-associated protein 1 light chain 3B.

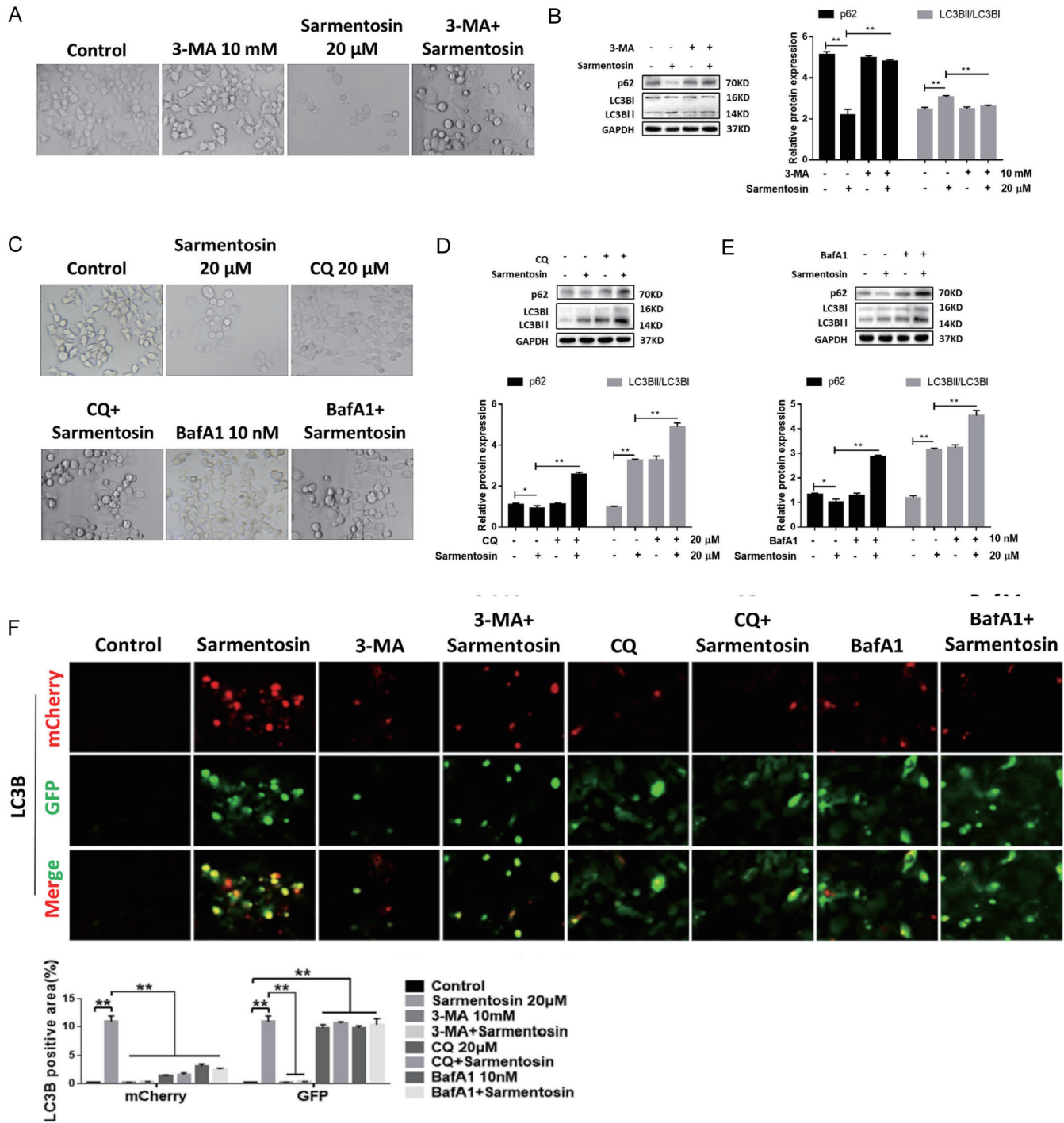


**Fig. 2. Sarmentosin activates autophagic flux in human HCC cells.** (A) Representative images of HepG2 cells obtained by optical microscopy show cell morphology and growth of HepG cells with or without 3-MA (10 mM) treatment for 1 h followed by the presence or absence of 6 h of sarmentosin (20 μM) treatment. *n*=10. (B) Western blotting and quantitative analysis showed the changes in LC3BII/II expression in HepG cells treated with or without 3-MA (10 mM) for 1 h followed by the presence or absence of 6 h of sarmentosin (20 μM) treatment. *n*=3, \*\**p*<0.01. (C) Representative images of HepG2 cells obtained by optical microscopy showed the cell morphology and growth in HepG cells treated with or without CQ (20 μM) or BafA1 (10 nM) for 1 h followed by the presence or absence of 6 h of sarmentosin (20 μM) treatment. *n*=10. (D) Western blotting and quantitative analysis shows the changes in LC3BII/II expression in HepG cells treated with or without CQ (20 μM) for 1 h followed by the presence or absence of 6 h of sarmentosin (20 μM) treatment. *n*=3, \*\**p*<0.01. (E) Western blotting and quantitative analysis show the changes in LC3BII/II expression in HepG cells treated with or without BafA1 (10 nM) for 1 h followed by the presence or absence of 6 sarmentosin (20 μM). *n*=3, \*\**p*<0.01. (F) After transfection with mCherry-GFP-LC3B in HepG2 cells, fluorescence microscopy was used to analyze LC3B expression in HepG2 cells treated with or without 3-MA (10 mM), CQ (20 μM), or BafA1 (10 nM) for 1 h followed by the presence or absence of 6 h of sarmentosin (20 μM) treatment. The LC3B-positive area percentage was calculated according to the fluorescent images. *n*=6, \*\**p*<0.01. CQ, chloroquine; HCC, hepatocellular carcinoma; LC3B, microtubule-associated protein 1 light chain 3B.

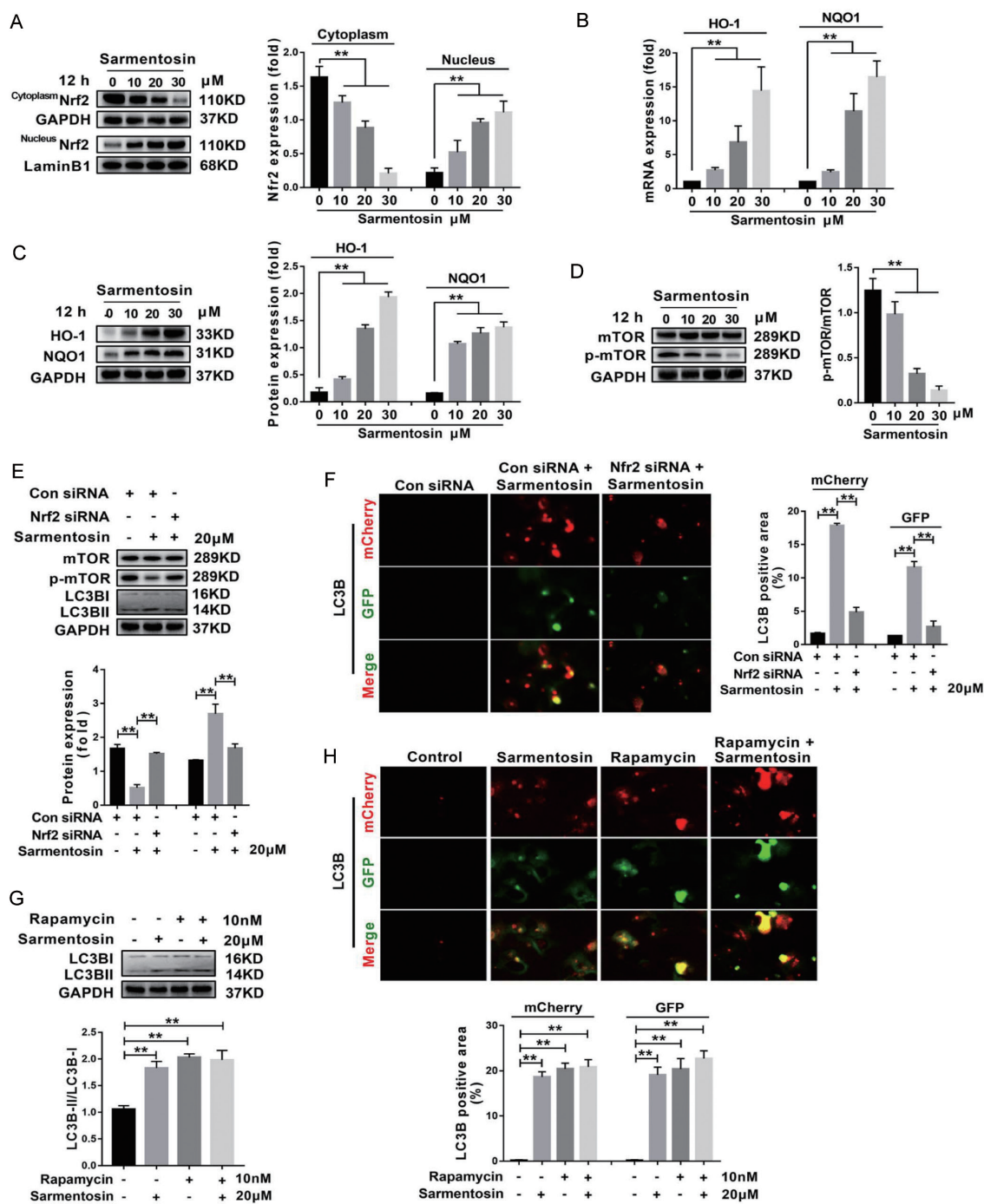


**Fig. 3. Nrf2 activation is required for sarmentosin to inhibit mTOR signaling and induce autophagy in human HCC cells.** (A) Western blotting and quantitative analysis show the changes in Nrf2 expression in the cytoplasm and nucleus of HepG cells treated with different concentrations of sarmentosin (10, 20, 30  $\mu$ M) for 12 h. *n*=3,  $**p < 0.01$ . (B) Real-time PCR was used to detect the changes in HO-1 and NQO1 mRNA expression in HepG cells treated with different concentrations of sarmentosin (10, 20, 30  $\mu$ M) for 12 h. *n*=6,  $**p < 0.01$ . (C) Western blotting and quantitative analysis shows the changes in HO-1 and NQO1 expression in HepG cells treated with different concentrations of sarmentosin (10, 20, 30  $\mu$ M) for 12 h. *n*=3,  $**p < 0.01$ . (D) Western blot and quantitative analysis showed the changes in mTOR and p-mTOR expression in HepG cells treated with different concentrations of sarmentosin (10, 20, 30  $\mu$ M) for 12 h. *n*=3,  $**p < 0.01$ . (E) Western blot and quantitative analysis shows the changes in mTOR, p-mTOR and LC3B-I/II expression in HepG2 cells transfected with Nrf2 siRNA or control siRNA followed by the presence or absence of 12 h of sarmentosin (20  $\mu$ M) treatment. *n*=3,  $**p < 0.01$ . (F) After transfection with mCherry-GFP-LC3B in HepG2 cells, fluorescence microscopy was used to analyze LC3B expression in HepG2 cells transfected with Nrf2 siRNA or control siRNA followed by the presence or absence of 12 h of sarmentosin (20  $\mu$ M) treatment. The LC3B-positive area percentage was calculated from fluorescence images. *n*=6,  $**p < 0.01$ . (G) Western blot and quantitative analysis showed the changes in LC3B-I/II expression in HepG2 cells treated with rapamycin (10 nM) and LC3B expression in HepG2 cells treated with rapamycin (10 nM) and sarmentosin (20  $\mu$ M) treatment. *n*=3,  $**p < 0.01$ . (H) After transfection with mCherry-GFP-LC3B in HepG2 cells, fluorescence microscopy was used to analyze LC3B expression in HepG2 cells treated with rapamycin (10 nM) and sarmentosin (20  $\mu$ M) treatment. *n*=6,  $**p < 0.01$ . HCC, hepatocellular carcinoma; LC3B, microtubule-associated protein 1 light chain 3B.

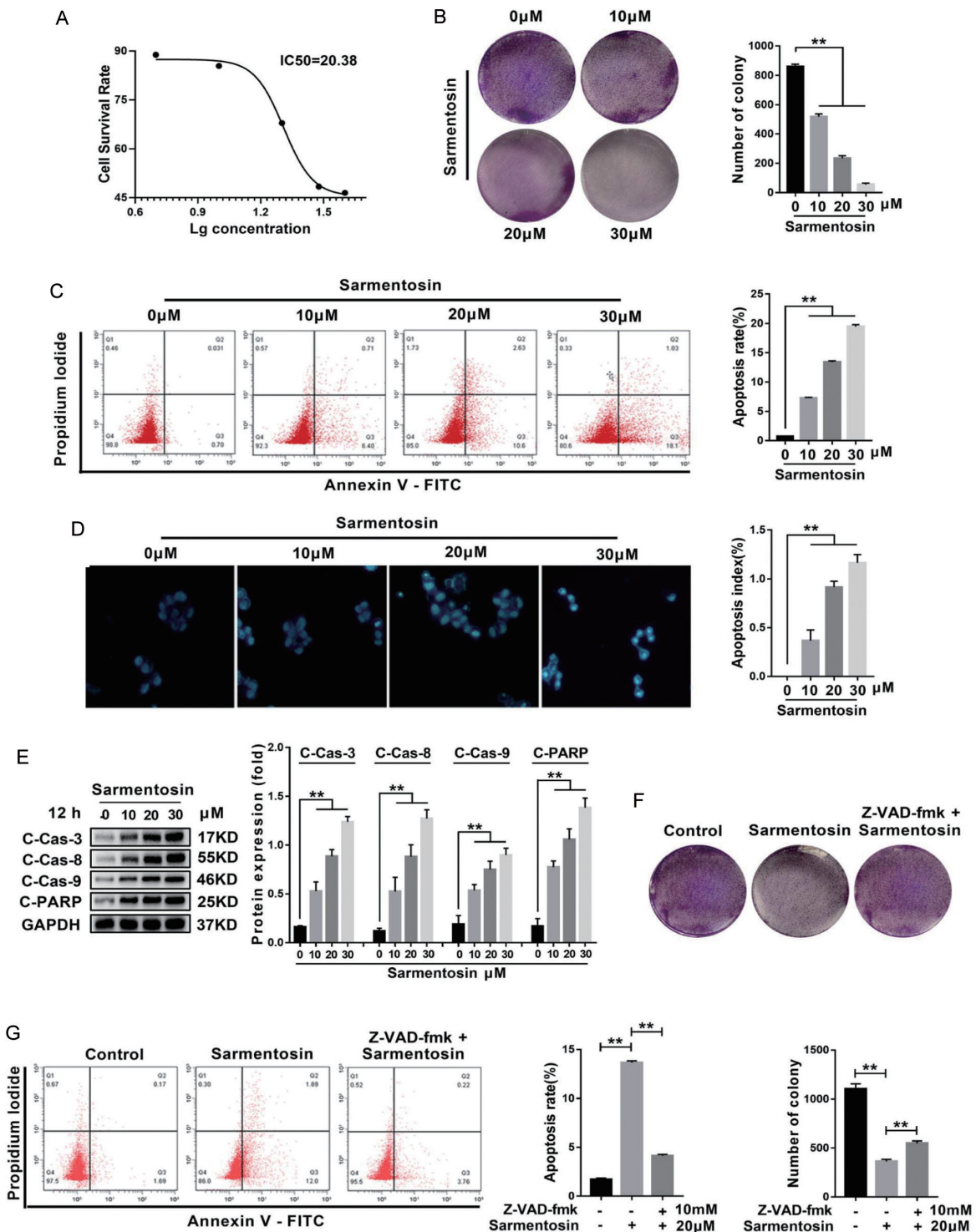


**Fig. 4. Sarmentosin stimulates caspase-dependent apoptosis in human HCC cells.** (A) Cell viability was measured by MTT assay, and  $IC_{50}$  values were calculated in HepG2 cells after 24 h of treatment with different concentrations of sarmentosin (5, 10, 20, 30, 40  $\mu$ M).  $n=10$ . (B) Cell cloning experiments and measurement were applied to HepG2 cells treated with different concentrations of sarmentosin (10, 20, 30  $\mu$ M).  $n=6$ ,  $**p<0.01$ . (C) Apoptosis was measured by flow cytometry in HepG2 cells after 12 h of treatment with different concentrations of sarmentosin (10, 20, 30  $\mu$ M).  $n=6$ ,  $**p<0.01$ . (D) Hoechst staining was used to detect and measure apoptosis in HepG2 cells after 12 h of treatment with different concentrations of sarmentosin (10, 20, 30  $\mu$ M).  $n=6$ ,  $**p<0.01$ . (E) Western blot and quantitative analysis showed the changes in cleaved caspase-3, cleaved caspase-8, cleaved caspase-9, and cleaved PARP expression in HepG2 cells after 12 h of treatment with different concentrations of sarmentosin (10, 20, 30  $\mu$ M).  $n=3$ ,  $**p<0.01$ . (F) Cell cloning experiments and measurement were performed in HepG2 cells treated with Z-VAD-fmk (10 mM) for 1 h followed by the presence or absence of sarmentosin (20  $\mu$ M).  $n=6$ ,  $**p<0.01$ . (G) Apoptosis was measured by flow cytometry and measured in HepG2 cells treated with Z-VAD-fmk (10 mM) for 1 h followed by the presence or absence of 12 h of sarmentosin (20  $\mu$ M) treatment.  $n=6$ ,  $**p<0.01$ . HCC, hepatocellular carcinoma.

lated apoptosis, as shown by flow cytometry analyses (Fig. 4C) and Hoechst staining (Fig. 4D). To confirm apoptosis, we examined several key molecules and found that the cleaved forms of caspase-8, caspase-9, caspase-3 and PARP were all increased by sarmentosin in a concentration-dependent manner (Fig. 4E). The caspase inhibitor Z-VAD-fmk was used to test whether sarmentosin-triggered cell death was caspase dependent. We saw that this compound considerably rescued sarmentosin-suppressed cell proliferation, as shown by colony-forming experiments (Fig. 4F), and abolished sarmentosin-induced apoptosis, as shown by flow cytometry (Fig. 4G). The above discoveries indicated that sarmentosin promoted caspase-dependent apoptosis in human HCC cells.

We then explored the role of autophagy and Nrf2 in sarmentosin-induced apoptosis. Cell colony-forming assays showed that CQ or siRNA-mediated knockdown of Nrf2 weakened the inhibitory effects of sarmentosin on cell proliferation (Fig. 5A). Flow cytometry showed that the increased apoptosis rate in sarmentosin-treated cells was abrogated by CQ or Nrf2 siRNA (Fig. 5B). In addition, the upregulation of the cleaved forms of caspase-8, caspase-9, caspase-3 and PARP was diminished by CQ or Nrf2 knockdown (Fig. 5C). To further confirm the requirement of autophagy in the current context, the key autophagy-related molecule ATG7 was depleted by transfection with its siRNA. As expected, knockdown of ATG7 eliminated the effects of sarmentosin on cell proliferation and apoptosis (Fig. 5D, E) and reduced the sarmentosin-induced activation of caspases and PARP (Fig. 5F). The above data suggest that sarmentosin-induced apoptosis in human HCC cells requires activation of Nrf2 and autophagy.

#### **Sarmentosin inhibits HCC in xenograft nude mice and is associated with the induction of autophagic apoptosis**

Finally, we investigated the *in vivo* relevance of the molecular findings in a culture system using xenograft mice. Mice bearing transplanted human HCC cells were treated with sarmentosin and sorafenib as a positive control for 21 days. We saw that sarmentosin at each time point reduced tumor volumes in a dose-dependent manner and that 5-fluorouracil produced the most significant effects (Fig. 6A). HE staining of tumor tissues revealed that the organization and architecture of tumor cells were destroyed by sarmentosin at different doses and 5-fluorouracil (Fig. 6B). TUNEL staining showed apoptotic HCC cells in sarmentosin- or 5-fluorouracil-treated mice (Fig. 6C). These observations indicated that sarmentosin inhibited HCC *in vivo*. Besides, the high dose of sarmentosin exhibits considerable effects on HepG2 cells as sorafenib *in vitro* (Supplementary Fig. 1B). We next confirmed the molecular events in tumor tissues. Western blot assay of cytoplasmic and nuclear lysates of tumor tissues showed that sarmentosin dose-dependently downregulated cytoplasmic Nrf2 abundance and upregulated nuclear Nrf2 levels (Fig. 7A). Sarmentosin also reduced mTOR phosphorylation and increased the levels of ATG7 and cleaved caspases (Fig. 7B, C). Compared with the model mice, sarmentosin at three doses decreased the levels of phosphorylated mTOR and increased the ATG7 and cleaved caspase-8, cleaved caspase-9, and cleaved caspase-3 in tumor tissues, as shown by immunohistochemical analyses (Fig. 7D). The observations followed the molecular discoveries in culture systems. Interestingly, the positive control drug 5-fluorouracil had similar effects in all the assessments. Given that selectivity and safety are critical features of an ideal anticancer agent, we also evaluated the effects of sarmentosin on body weight and several key organs. The obtained results showed that sarmentosin at three doses did not significantly change body

weights during the experiments (Supplementary Fig. 2A) and that the organization and structure of the heat, lung and kidney were not apparently altered by sarmentosin (Supplementary Fig. 2B). Taken together, the discoveries indicated that sarmentosin had potent and relatively safe anticancer activities against HCC *in vivo* associated with the induction of autophagic apoptosis.

#### **Discussion**

In this study, we demonstrated autophagy induced by sarmentosin in human HCC cells. To determine the exact role of autophagy in this setting, we used standard methods for assessing autophagic activity, including LC3B- and p62-based assays and electron microscopy,<sup>14</sup> and employed autophagy inhibitors at different stages. We saw a significantly increased LC3B-II/LC3B-I ratio and decreased p62 levels and accumulation of autophagosomes in HCC cells treated with sarmentosin for 12 h. More important, all three autophagy blockers abolished sarmentosin-induced autophagy. The observations indicated that sarmentosin promoted the conversion of the cytosolic form of LC3B-I to the autophagic membrane form of LC3B-II and enhanced autophagic activity according to the accumulation of p62 in HCC cells.

We then investigated how sarmentosin-induced autophagy affected cell death or survival. Interestingly, sarmentosin stimulated caspase-dependent apoptosis in HCC cells after 24 h of treatment exhibited considerable anti-HCC activity *in vitro*. We speculated that apoptosis could be a sequential consequence of autophagy, which was supported by the observation that blockade of autophagy remarkably abrogated sarmentosin-induced apoptosis in HCC cells. Sarmentosin modulated HCC cell fate via induction of autophagic apoptosis. Consistently, studies have shown that triggering autophagic apoptosis accounts for the anti-HCC effects of potential therapeutic compounds. For example, suppression of autophagy impaired crocin-induced apoptosis in HCC cells,<sup>15</sup> and autophagy served as an early step for  $\beta$ -thujaplicin induction of mitochondrial-dependent apoptosis in HepG2 cells.<sup>16</sup> Taken together, those findings and ours suggest that therapeutic stimulation of autophagy by natural compounds could be a promising strategy to treat HCC.

We next explored the upstream molecular events underlying the induction of autophagy-dependent apoptosis by sarmentosin in HCC cells. Given the increasing evidence highlighting a pivotal role for Nrf2 in the transcriptional regulatory network of cell death and survival,<sup>17</sup> we examined whether this master transcription factor was involved in the current context. Interestingly, we saw considerable activation of Nrf2 by sarmentosin in HCC cells. Then, loss-of-function analysis revealed that activation of Nrf2 was required for sarmentosin suppression of mTOR phosphorylation and induction of autophagic apoptosis. The positive role of Nrf2 in autophagy has been shown recently in many types of cancer cells. For example, Nrf2 induced autophagosome formation and enhanced autophagic activity in non-small cell lung cancer,<sup>18</sup> Nrf2 silencing inhibited autophagy in hypoxic breast cancer cells,<sup>19</sup> and highly autophagy-dependent cancer cells evolved to avoid the loss of autophagy by upregulating Nrf2.<sup>20</sup> Those findings were confirmed by our current findings in HCC cells.

We further revealed that mTOR was the linking molecule between Nrf2 and autophagy in sarmentosin-treated HCC cells, which was in accordance with the notion that mTOR activity is often inhibited to induce autophagy because it serves as a master sensor of nutrient, growth factor availability, energy levels, and stress signals.<sup>21</sup> It was shown that Nrf2 regulated autophagy via ubiquitination and proteasomal

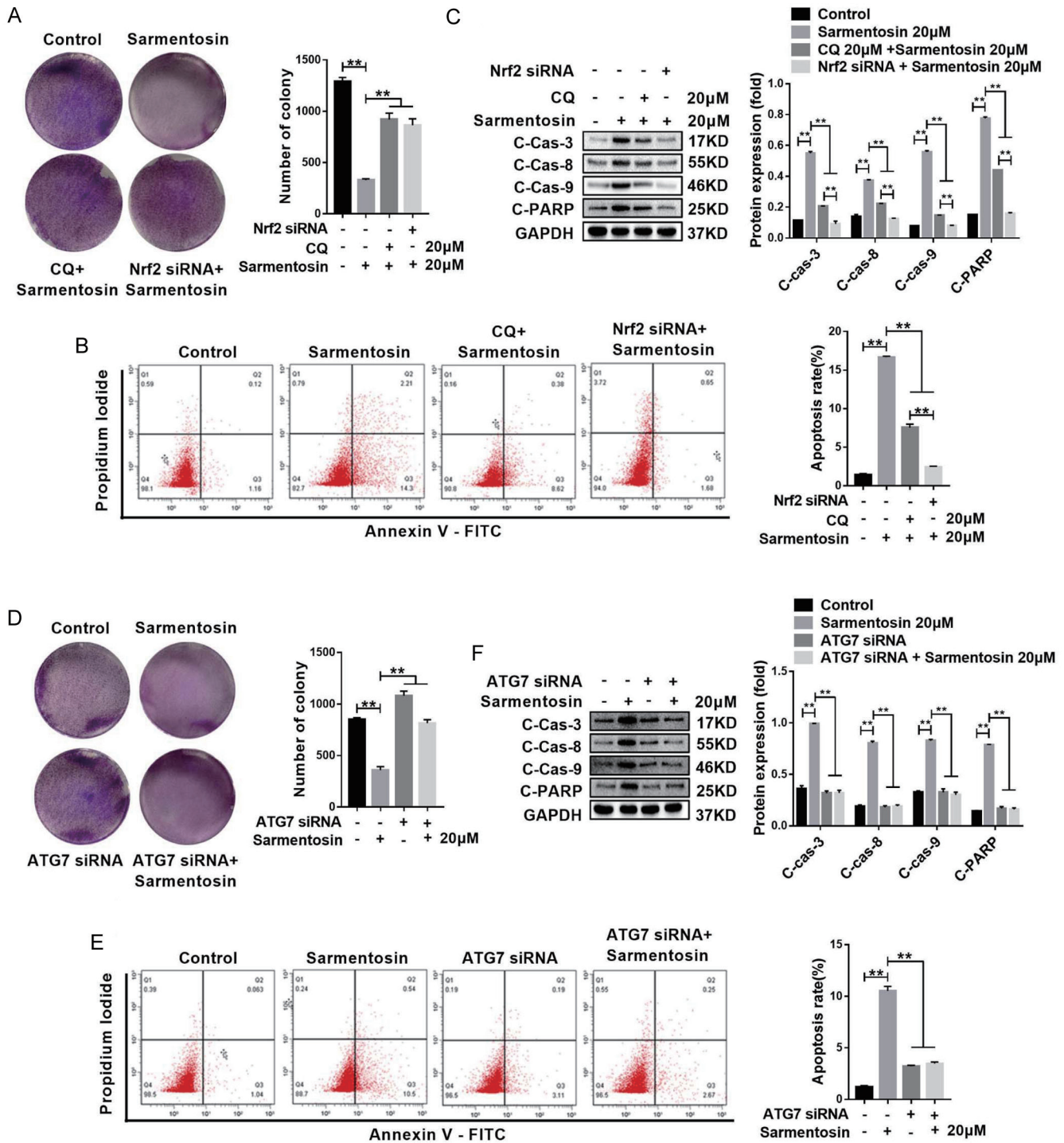


**Fig. 5. Activation of Nrf2 and autophagy is required for sarmentosin-induced apoptosis in HCC cells.** (A) Cell cloning experiments and measurement were applied in HepG2 cells transfected with Nrf2 siRNA or in HepG2 cells treated with CQ (20 µM) for 1 h followed by treatment with or without sarmentosin (20 µM).  $n=6$ ,  $**p<0.01$ . (B) Apoptosis was measured by flow cytometry and measured in HepG2 cells transfected with Nrf2 siRNA or in HepG2 cells treated with CQ (20 µM) for 1 h followed by the presence or absence of 12 h of sarmentosin (20 µM) treatment.  $n=6$ ,  $**p<0.01$ . (C) Western blot and quantitative analysis showed the changes in cleaved caspase-3, cleaved caspase-8, cleaved caspase-9, and cleaved PARP expression in HepG2 cells transfected with Nrf2 siRNA or in HepG2 cells treated with CQ (20 µM) for 1 h followed by the presence or absence of 12 h of sarmentosin (20 µM) treatment.  $n=3$ ,  $**p<0.01$ . (D) Cell cloning experiments and measurement were performed in HepG2 cells transfected with ATG7 siRNA followed by treatment with or without sarmentosin (20 µM). (E) Apoptosis was measured by flow cytometry and measured in HepG2 cells transfected with ATG7 siRNA followed by the presence or absence of 12 h of sarmentosin (20 µM) treatment.  $n=6$ ,  $**p<0.01$ . (F) Western blot and quantitative analysis shows the changes in cleaved caspase-3, cleaved caspase-8, cleaved caspase-9, and cleaved PARP expression in HepG2 cells transfected with ATG7 siRNA followed by the presence or absence of 12 h of sarmentosin (20 µM) treatment.  $n=3$ ,  $**p<0.01$ . ATG, autophagy-related gene; CQ, chloroquine; HCC, hepatocellular carcinoma.

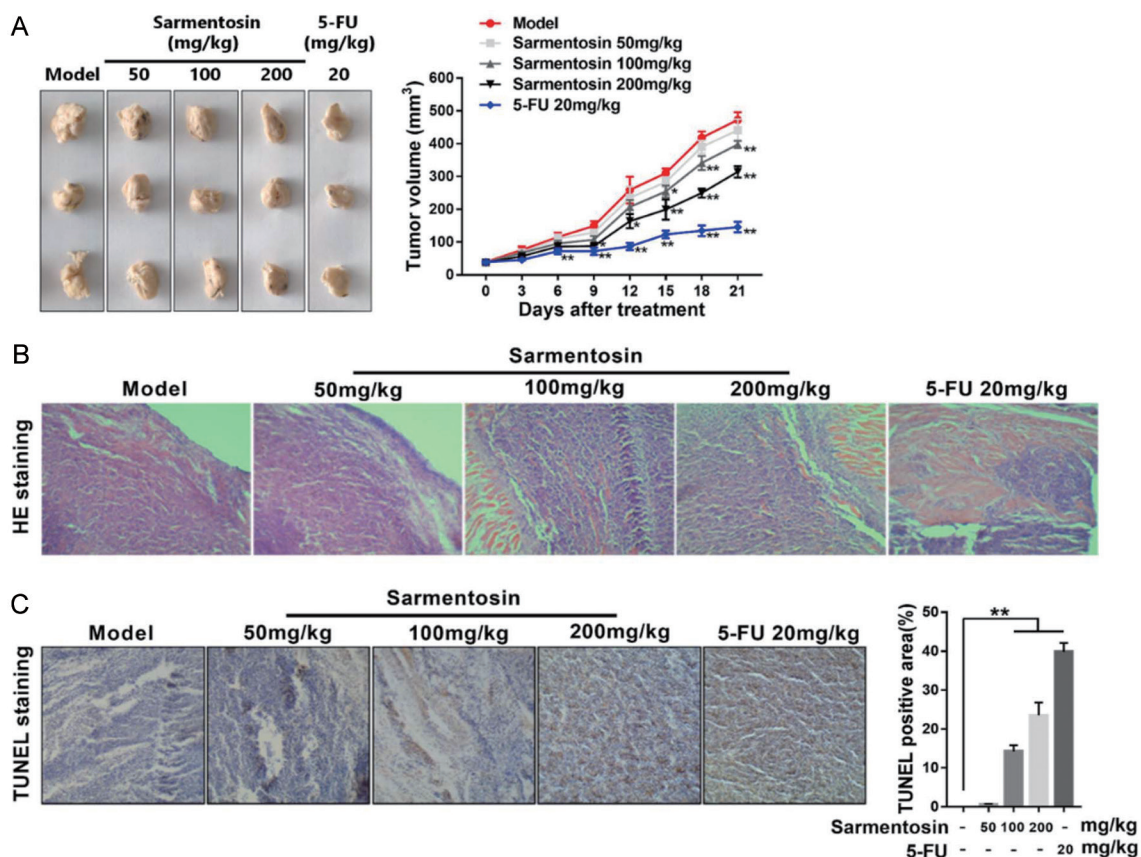


**Fig. 6. Sarmentosin inhibits HCC growth in xenografted nude mice.** (A) Paraformaldehyde-fixed tumors from xenograft nude mice in each group. Tumor volume was measured every 3 days in xenograft nude mice treated with or without different concentrations of sarmentosin (50, 100, 200 mg/kg) or 5-FU (20 mg/kg) for 21 days.  $n=6$ ,  $*p<0.05$ ,  $**p<0.01$ . (B) Representative images of HE staining of tumor sections from xenograft nude mice treated with or without different concentrations of sarmentosin (50, 100, 200 mg/kg) or 5-FU (20 mg/kg) for 21 days.  $n=6$ . (C) TUNEL staining was used to detect and measure apoptosis in tumor sections from xenograft nude mice treated with or without different concentrations of sarmentosin (50, 100, 200 mg/kg) or 5-FU (20 mg/kg) for 21 days.  $n=6$ ,  $**p<0.01$ . HCC, hepatocellular carcinoma.

degradation pathways and that each signaling pathway of autophagy depended on interactions between Nrf2 and ubiquitin proteins.<sup>22</sup> There was a high possibility that this mechanism might also be involved in the modulation of mTOR phosphorylation and autophagy by sarmentosin-activated Nrf2 in HCC cells. Different molecules interacting with Nrf2 could determine the transcriptional and posttranscriptional change state of downstream molecules.

The current paradigm suggests a controversial role for Nrf2 in apoptosis. The Nrf2-ARE pathway is an intrinsic mechanism of defense against oxidative stress. Nrf2 is a master transcription factor that upregulates the expression of a large number of cytoprotective and detoxifying genes.<sup>23</sup> Oxidative stress is a key inducer of apoptosis under many pathophysiological circumstances.<sup>24</sup> Inactivation of the Nrf2 pathway is often used to stimulate apoptosis. For example, antagonizing Nrf2 with its inhibitor brusatol was shown to increase the production of reactive oxygen species and elevate the expression of apoptosis-related proteins, which promoted neuronal apoptosis.<sup>25</sup> Atorvastatin induces mitochondrial dysfunction and apoptosis in HepG2 cells via disruption of the Nrf2 pathway.<sup>26</sup> Our current findings show that activation of Nrf2 was a prerequisite for sarmentosin-induced caspase-dependent apoptosis in HCC cells. The difference might be due to excessively enhanced autophagic activity followed by sarmentosin activation of Nrf2 that triggered the cell death

machinery. Under this situation, the presumed reduction in oxidative status due to Nrf2 activation was no longer a determining factor for cell fate decisions and could not rescue autophagy-dependent apoptotic death. Sarmentosin could likely be a potent autophagy stimulator rather than an antioxidant by targeting Nrf2 in HCC cells.

Finally, we provided clear *in vivo* evidence that sarmentosin inhibited HCC development by stimulating autophagy and apoptosis. All the molecular assays in HCC tissues were consistent with the results of the culture system. Sarmentosin at the selected doses was not toxic and had no side effects in nontumor tissues, which was a marked advantage for an antineoplastic chemotherapy drug. Everything has two sides, and autophagy is no exception. On one hand, autophagy generally increases cell viability as well as their resistance against endogenous or iatrogenic stress, so it has been widely proposed that inhibition of autophagy would be a valid strategy for sensitizing cancer cells to chemotherapy or radiotherapy.<sup>27</sup> But autophagosomes formation is the most important process of autophagy, followed by lysosomes decomposing damaged organelles. However, excessive autophagy can also damage normal organelles to preserve metastasis potential or even induce cancer cell death,<sup>28</sup> and it also provides the possibility that autophagy regulates the programmed cell death of cancer cells.

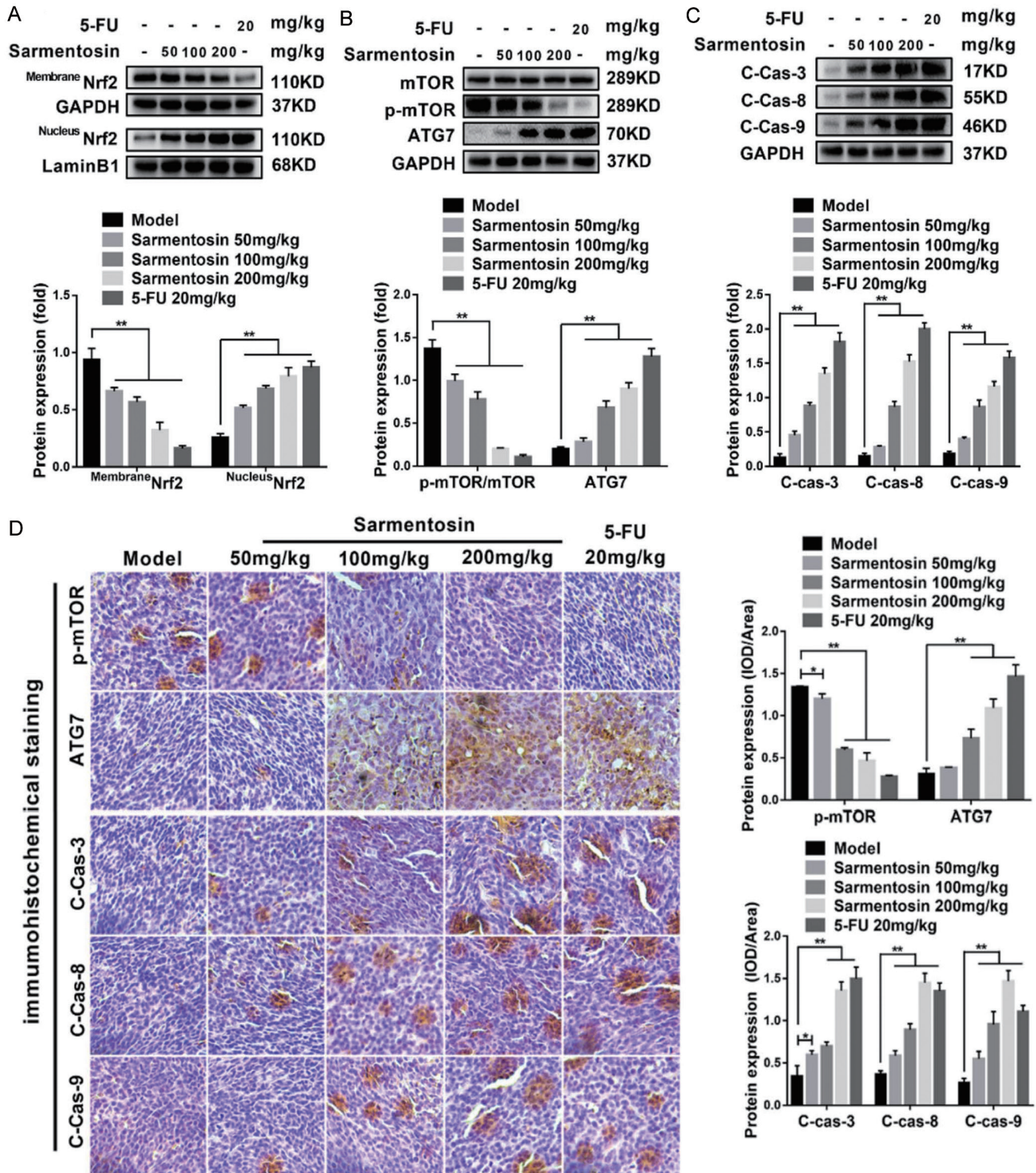


**Fig. 7. Sarmentosin regulates the Nrf2/mTOR axis and activates autophagic apoptosis in HCC in xenografted nude mice.** (A) Western blotting and quantitative analysis show the changes in Nrf2 expression in the cytoplasm and nucleus of tumors of xenograft nude mice treated with or without different concentrations of sarmentosin (50, 100, 200 mg/kg) or 5-FU (20 mg/kg) for 21 days.  $n=3$ ,  $**p<0.01$ . (B) Western blotting and quantitative analysis show the changes in mTOR, p-mTOR and Atg7 expression in tumors in xenograft nude mice treated with or without different concentrations of sarmentosin (50, 100, 200 mg/kg) or 5-FU (20 mg/kg) for 21 days.  $n=3$ ,  $**p<0.01$ . (C) Western blotting and quantitative analysis show the changes in cleaved caspase-3, cleaved caspase-8, and cleaved caspase-9 expression in tumors in xenograft nude mice treated with or without different concentrations of sarmentosin (50, 100, 200 mg/kg) or 5-FU (20 mg/kg) for 21 days.  $n=3$ ,  $**p<0.01$ . (D) Immunohistochemical staining was used to detect and measure p-mTOR, ATG7, cleaved caspase-3, cleaved caspase-8, and cleaved caspase-9 expression in tumor sections from xenograft nude mice treated with or without different concentrations of sarmentosin (50, 100, 200 mg/kg) or 5-FU (20 mg/kg) for 21 days.  $n=6$ ,  $*p<0.05$ ,  $**p<0.01$ . ATG, autophagy-related gene; HCC, hepatocellular carcinoma.

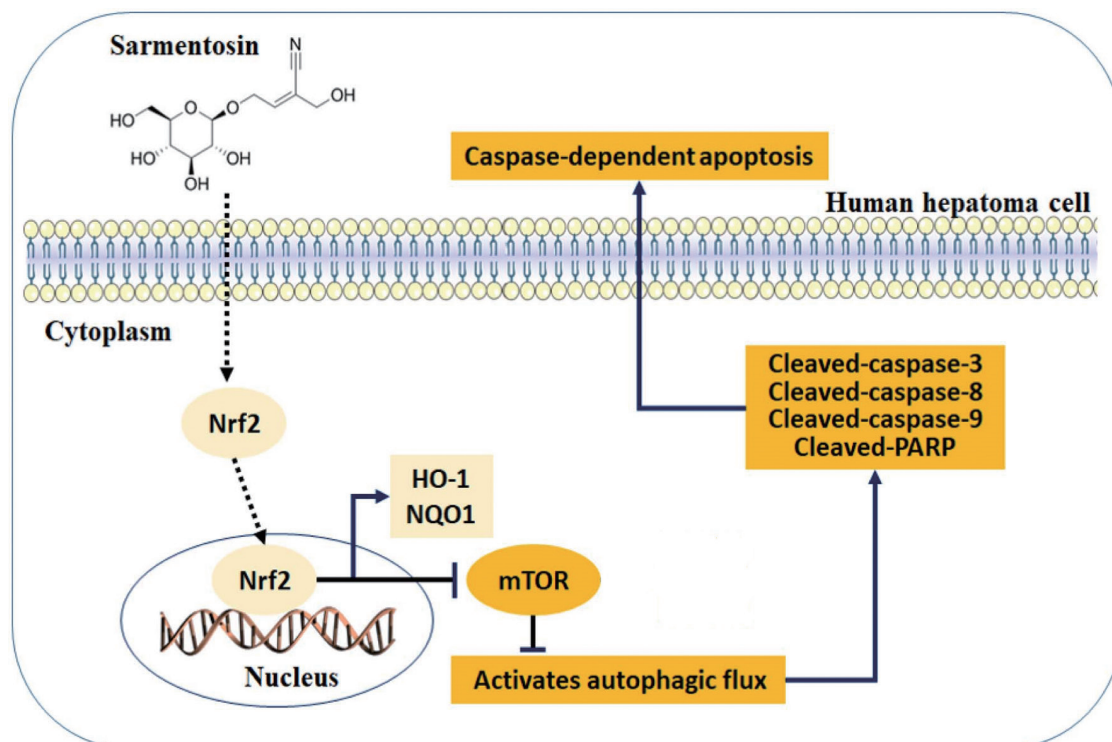


**Fig. 8. Illustration of the mechanism by which sarmentosin stimulated autophagy-dependent apoptosis in HCC cells.** HCC, hepatocellular carcinoma.

### Conclusion

We revealed that sarmentosin stimulated autophagy leading to caspase-dependent apoptosis in HCC cells. Its effects depended on the activation of Nrf2 and the resultant inhibition of mTOR (Fig. 8). Sarmentosin showed potent *in vivo* anti-HCC activity with high safety. Our data support Nrf2 as a therapeutic target for HCC and sarmentosin and as a promising candidate for HCC chemotherapy.

### Funding

This study was supported by grants from the financial support provided by Development Plan Project (SYSD2020221), the Fifth Batch of Suzhou Health Talents Project (GSWS2019075) and the Science and Technology Support Program of Jiangsu Province (BE2009682).

### Conflict of interest

The authors have no conflict of interests related to this publication.

### Author contributions

Conceived and designed the study (ZJ, JP), performed experiments and analyzed the data (ZJ, LG, CL), assisted in data interpretation and manuscript preparation (JW, YH), wrote the manuscript (ZJ), critical revision of the manuscript (JP), approved the final version of this manuscript (all authors).

### Ethical Statement

All animals were kept at the Experimental Animal Use Center of Nanjing University of Chinese Medicine, and the use of ani-

mals was approved by the Experimental Animal Ethics Committee of Nanjing University of Chinese Medicine.

### Data sharing statement

All data generated or analyzed during this study are included in this article.

### References

- [1] Parikh ND, Pillai A. Recent Advances in Hepatocellular Carcinoma Treatment. *Clin Gastroenterol Hepatol* 2021;19(10):2020–2024. doi:10.1016/j.cgh.2021.05.045, PMID:34116048.
- [2] Kishore SA, Bajwa R, Madoff DC. Embolotherapeutic Strategies for Hepatocellular Carcinoma: 2020 Update. *Cancers (Basel)* 2020;12(4):791. doi:10.3390/cancers12040791, PMID:32224882.
- [3] Amaral L, Spengler G, Molnar J. Identification of Important Compounds Isolated from Natural Sources that Have Activity Against Multidrug-resistant Cancer Cell Lines: Effects on Proliferation, Apoptotic Mechanism and the Efflux Pump Responsible for Multi-resistance Phenotype. *Anticancer Res* 2016;36(11):5665–5672. doi:10.21873/anticancer.11149, PMID:27793887.
- [4] Shimizu S, Yoshida T, Tsujioka M, Arakawa S. Autophagic cell death and cancer. *Int J Mol Sci* 2014;15(2):3145–3153. doi:10.3390/ijms15023145, PMID:24566140.
- [5] Acevo-Rodríguez PS, Maldonado G, Castro-Obregón S, Hernández G. Autophagy Regulation by the Translation Machinery and Its Implications in Cancer. *Front Oncol* 2020;10:322. doi:10.3389/fonc.2020.00322, PMID:32232004.
- [6] Lian LH, Jin X, Wu YL, Cai XF, Lee JJ, Nan JX. Hepatoprotective effects of Sedum sarmentosum on D-galactosamine/lipopolysaccharide-induced murine fulminant hepatic failure. *J Pharmacol Sci* 2010;114(2):147–157. doi:10.1254/jphs.10045fp, PMID:20838028.
- [7] Bjarnholt N, Nakonieczny M, Kędziorski A, Debinski DM, Matter SF, Olsen CE, *et al*. Occurrence of sarmentosin and other hydroxynitrile glucosides in *Parnassius* (papilionidae) butterflies and their food plants. *J Chem Ecol* 2012;38(5):525–537. doi:10.1007/s10886-012-0114-x, PMID:22527055.
- [8] Yan X, Zhou R, Ma Z. Autophagy-Cell Survival and Death. *Adv Exp Med Biol* 2019;1206:667–696. doi:10.1007/978-981-15-0602-4\_29, PMID:31777006.
- [9] Shimizu S. Autophagic Cell Death and Cancer Chemotherapeutics. In: Shimizu S, Nakao K, Minato N, Uemoto S (eds). *Innovative Medicine: Basic Research and Development*. Tokyo: Springer; 2015:219–226.

- [10] Linder B, Kögel D. Autophagy in Cancer Cell Death. *Biology (Basel)* 2019;8(4):82. doi:10.3390/biology8040082, PMID:31671879.
- [11] Cuomo F, Altucci L, Cobellis G. Autophagy Function and Dysfunction: Potential Drugs as Anti-Cancer Therapy. *Cancers (Basel)* 2019;11(10):1465. doi:10.3390/cancers11101465, PMID:31569540.
- [12] Mai S, Muster B, Bereiter-Hahn J, Jendrach M. Autophagy proteins LC3B, ATG5 and ATG12 participate in quality control after mitochondrial damage and influence lifespan. *Autophagy* 2012;8(1):47–62. doi:10.4161/auto.8.1.18174, PMID:22170153.
- [13] Pasquier B. Autophagy inhibitors. *Cell Mol Life Sci* 2016;73(5):985–1001. doi:10.1007/s00018-015-2104-y, PMID:26658914.
- [14] Singh B, Bhaskar S. Methods for Detection of Autophagy in Mammalian Cells. *Methods Mol Biol* 2019;2045:245–258. doi:10.1007/7651\_2018\_190, PMID:30242567.
- [15] Yao C, Liu BB, Qian XD, Li LQ, Cao HB, Guo QS, *et al*. Crocin induces autophagic apoptosis in hepatocellular carcinoma by inhibiting Akt/mTOR activity. *Onco Targets Ther* 2018;11:2017–2028. doi:10.2147/OTT.S154586, PMID:29670377.
- [16] Zhang G, He J, Ye X, Zhu J, Hu X, Shen M, *et al*.  $\beta$ -Thujaplicin induces autophagic cell death, apoptosis, and cell cycle arrest through ROS-mediated Akt and p38/ERK MAPK signaling in human hepatocellular carcinoma. *Cell Death Dis* 2019;10(4):255. doi:10.1038/s41419-019-1492-6, PMID:30874538.
- [17] Murakami S, Motohashi H. Roles of Nrf2 in cell proliferation and differentiation. *Free Radic Biol Med* 2015;88(Pt B):168–178. doi:10.1016/j.freeradbiomed.2015.06.030, PMID:26119783.
- [18] Wang J, Liu Z, Hu T, Han L, Yu S, Yao Y, *et al*. Nrf2 promotes progression of non-small cell lung cancer through activating autophagy. *Cell Cycle* 2017;16(11):1053–1062. doi:10.1080/15384101.2017.1312224, PMID:28402166.
- [19] Lee S, Hallis SP, Jung KA, Ryu D, Kwak MK. Impairment of HIF-1 $\alpha$ -mediated metabolic adaptation by NRF2-silencing in breast cancer cells. *Redox Biol* 2019;24:101210. doi:10.1016/j.redox.2019.101210, PMID:31078780.
- [20] Towers CG, Fitzwalter BE, Regan D, Goodspeed A, Morgan MJ, Liu CW, *et al*. Cancer Cells Upregulate NRF2 Signaling to Adapt to Autophagy Inhibition. *Dev Cell* 2019;50(6):690–703.e6. doi:10.1016/j.devcel.2019.07.010, PMID:31378590.
- [21] Kim YC, Guan KL. mTOR: a pharmacologic target for autophagy regulation. *J Clin Invest* 2015;125(1):25–32. doi:10.1172/JCI73939, PMID:25654547.
- [22] Jiang T, Harder B, Rojo de la Vega M, Wong PK, Chapman E, Zhang DD. p62 links autophagy and Nrf2 signaling. *Free Radic Biol Med* 2015;88(Pt B):199–204. doi:10.1016/j.freeradbiomed.2015.06.014, PMID:26117325.
- [23] Buendia I, Michalska P, Navarro E, Gameiro I, Egea J, León R. Nrf2-ARE pathway: An emerging target against oxidative stress and neuroinflammation in neurodegenerative diseases. *Pharmacol Ther* 2016;157:84–104. doi:10.1016/j.pharmthera.2015.11.003, PMID:26617217.
- [24] Radi E, Formichi P, Battisti C, Federico A. Apoptosis and oxidative stress in neurodegenerative diseases. *J Alzheimers Dis* 2014;42(Suppl 3):S125–S152. doi:10.3233/JAD-132738, PMID:25056458.
- [25] Sun P, Nie X, Chen X, Yin L, Luo J, Sun L, *et al*. Nrf2 Signaling Elicits a Neuroprotective Role Against PFOS-mediated Oxidative Damage and Apoptosis. *Neurochem Res* 2018;43(12):2446–2459. doi:10.1007/s11064-018-2672-y, PMID:30382449.
- [26] Li LZ, Zhao ZM, Zhang L, He J, Zhang TF, Guo JB, *et al*. Atorvastatin induces mitochondrial dysfunction and cell apoptosis in HepG2 cells via inhibition of the Nrf2 pathway. *J Appl Toxicol* 2019;39(10):1394–1404. doi:10.1002/jat.3825, PMID:31423616.
- [27] Xing Y, Wei X, Liu Y, Wang MM, Sui Z, Wang X, *et al*. Autophagy inhibition mediated by MCOLN1/TRPML1 suppresses cancer metastasis via regulating a ROS-driven TP53/p53 pathway. *Autophagy* 2022;18(8):1932–1954. doi:10.1080/15548627.2021.2008752, PMID:34878954.
- [28] Li X, Yang KB, Chen W, Mai J, Wu XQ, Sun T, *et al*. CUL3 (cullin 3)-mediated ubiquitination and degradation of BECN1 (beclin 1) inhibit autophagy and promote tumor progression. *Autophagy* 2021;17(12):4323–4340. doi:10.1080/15548627.2021.1912270, PMID:33977871.